Simultaneous measurements of PIV, anisole-PLIF and OH-PLIF for investigating back-supported stratified flame propagation in lean and nonflammable mixtures

E. Delangle, B. Lecordier, C. Lacour, A. Cessou

Simultaneous measurements of PIV, anisole-PLIF and OH-PLIF for investigating back-supported stratified flame propagation in lean and nonflammable mixtures

E. DELANGLE[1], B. LECORDIER[1], C. LACOUR[1], A. CESSOU[1*]
1: CORIA-UMR6614, Normandie Université, CNRS, INSA and Université de Rouen, France
* Correspondent author: Armelle.cessou@coria.fr

Keywords: PIV; anisole-PLIF; OH-PLIF, combustion, laminar stratified flames, nonflammable mixture, memory effect

ABSTRACT

In an effort to reduce pollutant emissions and increase energy efficiency, partially premixed combustion has been integrated into many new combustion technologies. The present study investigated lean back-supported flames in a stratified combustion regime. This strategy leads to hybrid combustion regimes, ranging between fully premixed and fully non-premixed reactants, with a large panel of flame structures and properties requiring to be characterized. Outwardly propagating flames were observed following ignition under laminar stratification conditions generated in a constant volume vessel. The quantitative analysis of the flame properties relied on simultaneous PIV measurements to obtain local flame burning velocities and stretch rates and used anisole-PLIF measurements to calculate the equivalence ratio. Simultaneous OH-PLIF measurements were used to differentiate between the burned gas boundaries and the active flame front. This differentiation was necessary to investigate the nonflammable mixture. The OH-gradient measurement proved to be suitable for distinguishing burned gas interfaces from active flame fronts. Simultaneous OH- and anisole-PLIF measurements were used to estimate the thermal flame thickness. Two flame families were investigated: in family A the flame was ignited in a lean mixture (φ=0.6) with a rich stratification; in family B the mixture in the chamber was nonflammable. In rich mixtures ignition compensated for the non-equidiffusive effects of the lean propane flame and reinforced the flame's stretch resistance. Both a flammable and a nonflammable mixture were investigated to determine the time scales of the back-supported propagation for the given stratification. The enhanced combustion regime allowed the flame to propagate with an active flame front, even in the nonflammable mixture. Combustion continued for a few milliseconds before the flame extinguished. The richer the stratification, the longer the combustion lasted in the nonflammable mixture.

1. Introduction

Partially premixed combustion is intentionally introduced in many new combustion technologies to reduce pollutant emission or increase energetic efficiency. This strategy leads to hybrid combustion regimes, ranging between fully premixed and fully non-premixed reactants, with a large panel of flame structures and properties requiring to be characterized. The paper

investigates stratified flames, which concerns premixed combustion with compositionally inhomogeneous mixture where the flame succeeds to propagate (Masri 2015). In the purpose of investigating lean back-supported flames by stratified combustion and of focusing on flames propagating towards lean non-flammable mixtures, the present paper presents a combination of simultaneous diagnostics: PIV, anisole-PLIF, OH-PLIF, and proposes a new measurement of flame thickness directly linked to the thermal flame thickness. These simultaneous diagnostics provide various flame properties like burning velocity, stretch rate, equivalence ratio and velocity fields in fresh gases, flame thickness and identification of the active flame front. These quantities are of major interest for investigating lean back-supported flames, where stratified combustion leads to enhancement of burning rate (Jiménez 2002, Marzouk et al. 2000, Richardson et al. 2010), heat release (Zhou and Hochgreb 2013), thinner flame thickness (Richardson, Granet, Eyssartier and Chen 2010), extended flammable limits (Kang and Kyritsis 2007, Marzouk, Ghoniem and Najm 2000) and better resistance to stretch (Balusamy et al. 2014). Even if experimental and numerical investigations conclude that these effects are due to additional temperature of burned gas and species flux from products (Marzouk, Ghoniem and Najm 2000, Pires da Cruz 2000), these flames still suffered from incomplete understanding.

The flames investigated consist in outwardly propagating flames. This flame configuration is chosen since it is a well-established and extensively used method for measuring burning velocity in homogeneous mixture and is convenient for the direct determination of stretch rate (Egolfopoulos et al. 2014). In this configuration the burning velocity is often deduced from the measurement of the flame speed, S_b displacement speed of the burned gas, using the assumptions of stationary burned gas and of the knowledge of the burned gas temperature. For inhomogeneous mixtures these assumptions are not valid anymore, but the direct measurement of burning velocity (Balusamy et al. 2011) can be performed from the determination of the displacement speed with respect to the unburned gas, U_n, determined as S_b-U_g (Andrews and Bradley 1972, Bradley 1996), where U_g is the maximum velocity upstream of the flame. The flames are outwardly propagating after ignition in the middle of laminar stratifications generated in a constant volume vessel. The analysis is conducted once the flame propagates in the lean homogenous mixture after having been ignited in richer mixture as in a previous work (Balusamy, Cessou and Lecordier 2014). OH-PLIF is implemented for investigation in non-flammable mixture, where the distinction between burned gas boundaries and active flame front is required. It is shown that OH-gradient measurement is suitable for distinguishing burned gas interfaces from active flame front. Simultaneous OH and anisole PLIF provides an estimation of the thermal flame thickness. The interest of all the laser diagnostic measurements is shown by presenting the flame properties for various amplitudes of the stratified layers.

2. Experimental setup

The optical setup is presented in Figure 1. The PIV setup consisted of a double-cavity Nd:YAG laser (Twins Ultra, Quantel), delivering pulses of 30 mJ at 532 nm, and a full-frame interline CCD camera (Hamamatsu C9300) that was equipped with a Nikkor lens (135mm, f/dmax = 2, f/8) and provided a 12-bit image pair of 2048×2048 pixels. The anisole-PLIF setup used a fourth harmonic generator with an Nd:YAG laser (Quantel, YG180) that delivered 30 mJ of power to ensure a linear regime. A dye laser (Quantel, TDL90) (20 mJ) pumped by a second harmonic generator with an Nd:YAG laser (Quantel, Brillant B) was used as the OH-PLIF laser source. Both LIF radiation measurements were collected with intensified CCD cameras (Roper Scientific PIMAX512), equipped with a 98 mm UV lens (CERCO 2178, SODERN, f/2.8)) for anisole-PLIF and a 105 mm lens (Nikkor 105, f/4.5) for OH-PLIF. Dichroic mirrors were used to optically combine the three laser beams, and the overlapping laser sheets were formed by combining a spherical (f = 1 m) lens with two cylindrical lenses (f = −25 mm, f = +100 mm).

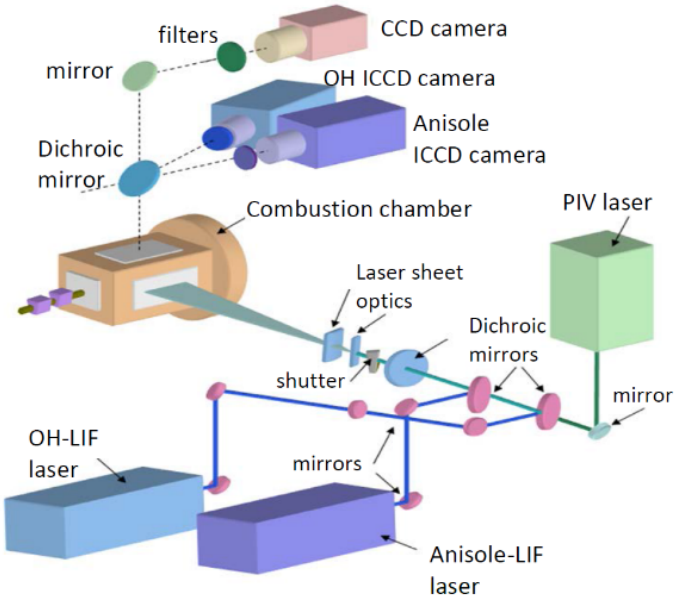

Fig 1 Experimental setup

The airflow was seeded with olive oil particles, and the propane flow was seeded with anisole (0.015% in volume in the stoichiometric propane–air mixture). OH–PLIF images were corrected for laser sheet inhomogeneities by collecting a LIF reference image obtained from homogeneous images of a rich propane–air mixture seeded with anisole. PIV and LIF radiations were separated with a dichroic mirror, which had a cut-off wavelength of 350 nm. Fluorescence was collected for anisole in the spectral range of 275 to 350 nm with a 10 mm thick liquid filter (0.6% vol. of

toluene in iso-octane) and with a combination of Schott filters (UG11 and WG280, 3 mm). The time delay between the two PIV pulses was adjusted to the velocity magnitude. The PLIF laser pulses were fired at intervals of 2 μs and positioned in the middle of the PIV time delay at intervals of 2 μs. A calibration grid was used to determine the high-order mapping functions of the three cameras (Figure 2). This calibration ensured the perfect overlap of the three measurements, especially for the OH-PLIF off-axis acquisition, which viewed the laser sheet at a slightly tilted angle.

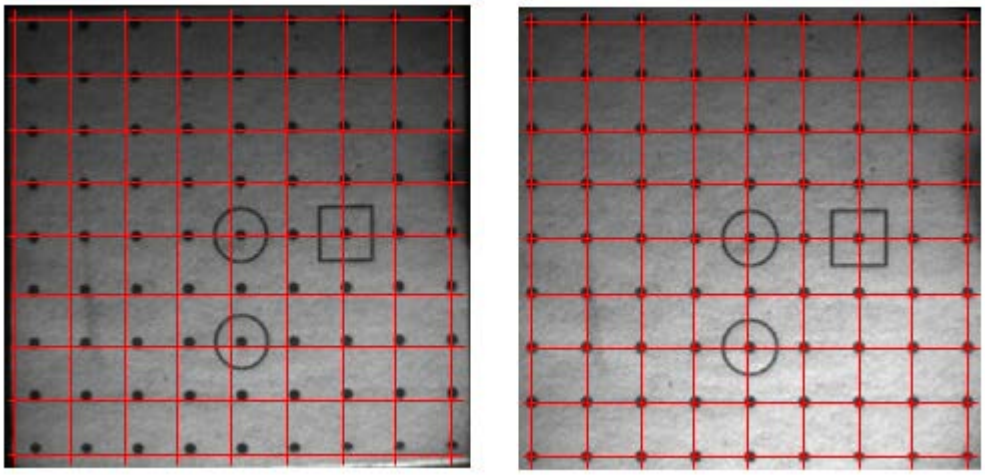

Fig 2 regular grid superimposed to raw grid image (left), corrected grid image (right)

Experiments were conducted in a 60×60×160 mm^3 constant volume combustion chamber equipped with three quartz windows, allowing optical access in the visible and UV spectra. The chamber was initially filled with a lean homogeneous propane–air mixture with either φ=0.6 or φ=0.4 at atmospheric pressure. The stratified mixture field was created by injecting a laminar jet of a richer mixture into the chamber with an injection system, providing controllable and repeatable mixture stratifications. Two flame families were investigated (Table 1): Family A, where the flame was ignited in a rich stratification with a lean mixture of φ_{ch}=0.6, corresponding to a mixture at the border of the flammability limit. Family B, where the mixture in the chamber was φch=0.4, below flammability limit, and flames were ignited in several richer mixtures from φ_ig=0.8 to φ_ig=1.5.

The stratified mixture was spark-ignited by energizing two thin electrodes with a diameter of 0.4 mm placed at the center of the combustion chamber. Previous experiments on homogeneous mixtures in this combustion chamber have shown that spark energy and electrode heat loss did not affect flame propagation. The limited volume of the chamber had little influence on flame propagation for the investigated time frame (with a pressure increase of less than 40 mbar), and due to the direct measurement procedure used for its determination the burning velocity

measurement is non-affected by the limited chamber volume (Balusamy, Cessou and Lecordier 2011).

Table 1. Investigated flame families:
mixture at rest in chamber (φ_{ch}); equivalence ratio at ignition (φ_{ig})

		φ_{ig}			
	φ_{ch}	0.8	1.0	1.2	1.5
Family A	0.6			1.2–0.6	1.5–0.6
	0.7			1.2–0.7	
Family B	0.4	0.8–0.4	1.0–0.4	1.2–0.4	1.5–0.4

3. Results and discussion

Active flame front identification

Once the flame reached the nonflammable mixture, φ_{ch}=0.4, it became necessary to differentiate between the burned gas boundaries and the active flame front. For the interface of fresh and burned gas, numerous studies have proposed to use OH-gradient levels to identify flame fronts (Bayley et al. 2010, Sadanandan et al. 2008, Sweeney and Hochgreb 2009). After obtaining the OH outline, the OH signal was extracted along its normal. This normal profile was interpolated with a complementary error function (erfc) before calculating the noise-free gradient (Figure 3).

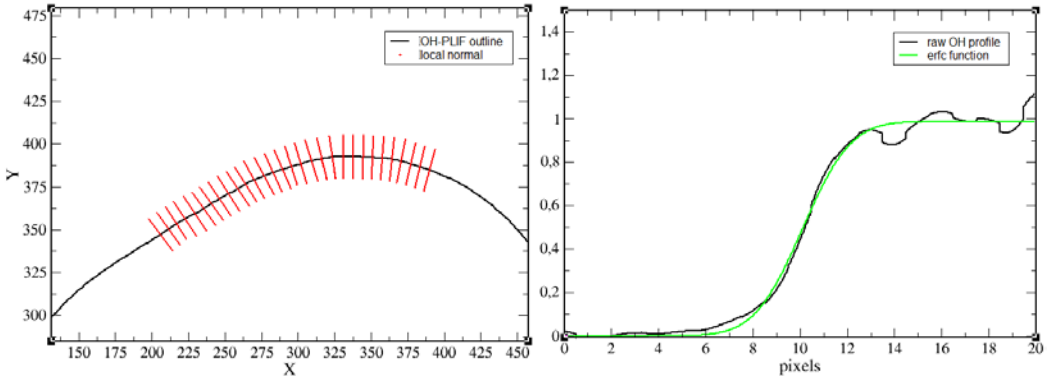

Fig 3 example of erfc function extraction from a local

To ensure that OH-gradient levels are suitable for determining active flame fronts, OH-gradient mapping was first compared with OH×CH_2O PLIF to verify that this simple diagnostic was sufficiently able to localize local flame extinctions. This preliminary experiment is performed in a Bunsen burner conical flame, where a local extinction was produced by a small air jet. In Fig. 4, a threshold value of OH-gradient is visible where the flame is extinguished. The value of this threshold value was determined for homogeneous outwardly propagating flame.

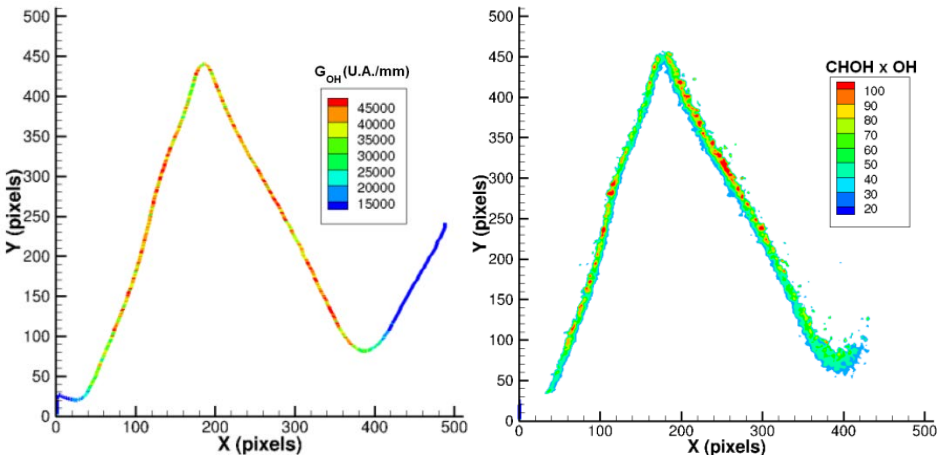

Fig 4 simultaneous OH-gradient and CH2OxOH LIF in a Bunsen burner conical flame, where a local extinction is made by injection a small air jet.

Then, the OH-gradient threshold was defined (in arbitrary units) to provide the critical limit below which the flame extinguished. The OH gradient has previously been measured for homogenous outwardly propagating flames at various equivalence ratios of up to φ = 0.6., while in the present configuration, the flame kernel could not self-propagate below φ = 0.62. Figure 5 shows the probability density functions (PDF) of the OH gradient according to equivalence ratio.

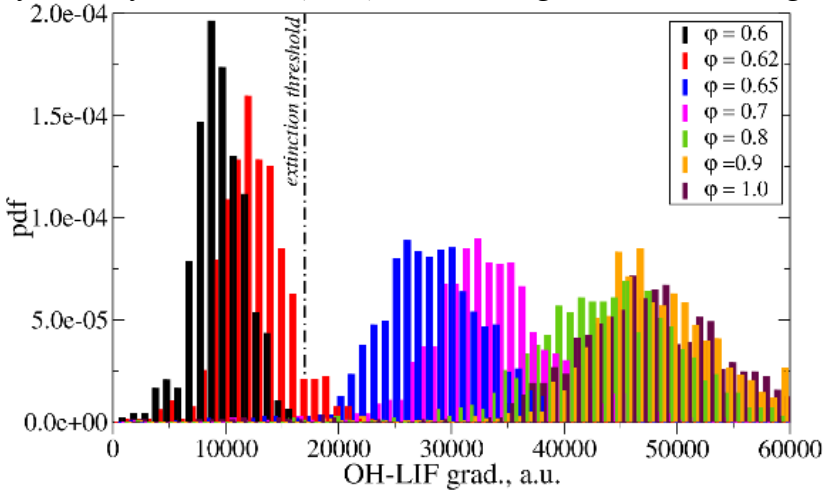

Fig 5 Probability density function of OH-PLIF gradient normal to the PLIF outline

The peak values decreased from the stoichiometric mixture to the lean composition. The flames with the two lowest equivalence ratios (φ = 0.6 and φ = 0.62), for which the homogenous flame could not self-propagate, presented PDFs clearly separated from the others. Thus, the critical threshold was defined as 17 000 a.u, after correcting the laser sheet profile. This gradient calculation procedure was used to obtain the OH-PLIF gradient of the stratified flames.

Flame thickness determination

The equivalence ratio was measured based on anisole-PLIF, following a shot-to-shot laser sheet correction according to the procedure outlined by Balusamy et al. (Balusamy, Cessou and Lecordier 2014). The OH-PLIF marked high temperature burned gas (T>1500 K), whereas anisole pyrolysis was noticeable around 800 K (Nowakowska et al. 2014). After calibrating the mapping functions of the three cameras, the distance between these two isotherms, determined by superpositioning the simultaneous OH-PLIF and anisole-PLIF measurements, was used to define a thickness labeled δ_{LIF}. The local distance between these two isotherms is measured all around the flame outline from the superposition of the simultaneous OH-PLIF and anisole-PLIF. It varies with the stratification (Figure 6).

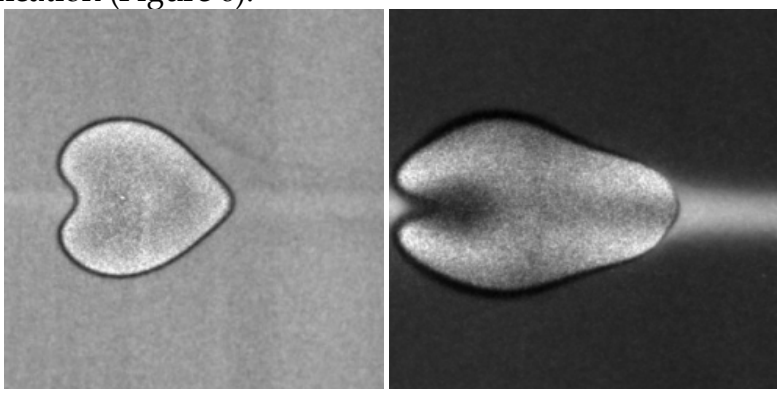

Fig 6 superposition of the simultaneous OH-PLIF and anisole-PLIF for the homogeneous laminar jet at $\varphi_{ig} = 0.8$ to $\varphi_{ch} = 0.8$, 4 ms after ignition (left) and for the case $\varphi_{ig} = 1.2$ to $\varphi_{ch} = 0.4$ (right)

Figure 7 shows a comparison of δ_{LIF} values obtained for different homogeneous flames with the thermal thickness $\delta_{th} = (T_b - T_u)/\nabla T_{max}$, calculated by modeling the unstretched 1D propane–air flame carried out by Cantera (Goodwin et al. 2015) and the chemical scheme provided by Jerzembeck et al. (Jerzembeck et al. 2009). The similarity of the resulting values shows that δ_{LIF} can be used to estimate the local flame thickness. δ_{LIF} can also be compared to the distance for an isotherm chosen to mark the disappearance of anisole and the location of $\nabla[OH]_{max}$ in the temperature profile of the numerical flame model, as a first modeling tentative of the measurement. This distance is shown in Fig 7 for the 650K-isotherm. This first result is coherent with the order of magnitude of pyrolysis temperature of anisole and motivates for future work to introduce the kinetics of anisole pyrolysis in the flame modeling and to verify if δ_{LIF} can be used quantatively as a thickness of the reaction progress. In the present work, δ_{LIF} is used for approximate estimation of the thermal thickness. Stratified flame measurements were compared with the values obtained for homogeneous flames.

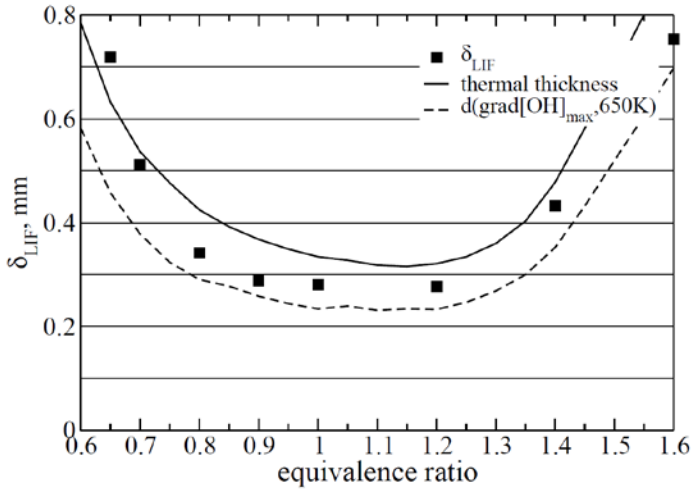

Fig 7 Thickness according to equivalence ratio: comparison of δ_{LIF} with the thermal thickness given by the plane flame calculation for propane–air, the distance between the isotherm 650K and the line of $\nabla[OH]_{max}$ in the flame modeling

Flame properties in the stratified flows

The criterion on OH-PLIF gradient and the flame thickness measurement are used to analyze the flame behavior for the two families investigated. These new measurements are combined with the measurements of burning velocity and stretch rates measured all around the stratified flames from the procedure of Balusamy et al (Balusamy et al. 2011), providing a direct measurement based on the difference between the local flame speed and the fresh gas velocity at the entrance of the preheat zone. The flame properties were analyzed after the flame began propagating in the lean homogeneous mixture filling the combustion chamber—that is, for $t \geq 2\ ms$. To limit the analysis to conditions comparable to outwardly propagating flames in a homogeneous mixture, the conditional analysis relied on the same criteria as used by Balusamy et al. (Balusamy, Cessou and Lecordier 2014): Measurements were conditioned on the equivalence ratio in the chamber, ($\varphi_{ch} = \pm 0.05$) and the moderate tangential velocity (−5% to 5% of the U_g average). An additional condition limited the investigation to flame segments propagating almost perpendicularly to the stratified layer: an angular sector of ±20° from the ignition location was chosen (Fig 8). This angular condition restricted the flame analysis to segments mainly exposed to the flame curvature effect with limited flow non-uniformity influences and with almost the same residence time in the homogeneous lean mixture. Given these new criteria, sampling was restricted to flame segments with an almost constant stretch rate at every moment after ignition. Consequently, the stretch rate was averaged at each time, and the flame properties were not extrapolated to a zero stretch rate, as done by Balusamy et al. (Balusamy, Cessou and Lecordier 2014).

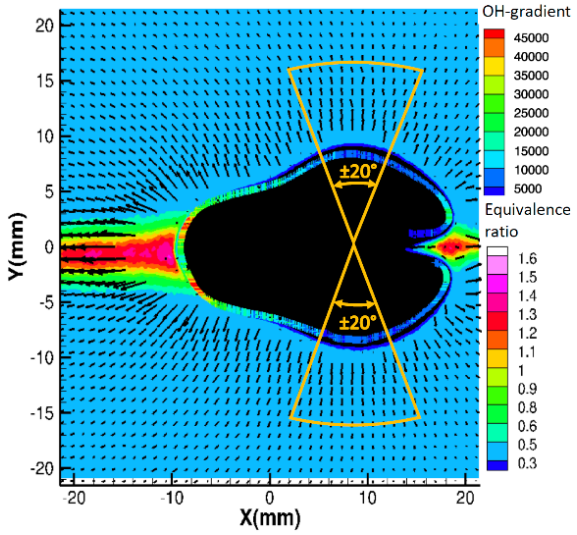

Fig 8 Combined measurements and angular sector of the conditional analysis

Family A: propagation in the lean flammable mixture

Figure 9 presents the burning velocity according to time. The unstretched velocity was $U_n^\circ = 0.12\ m/s$ for $\varphi = 0.6$ and $U_n^\circ = 0.20\ m/s$ for $\varphi =$ 0.7, thus the expected burning velocity for stretched velocities should be lower due to negative thermodiffusive effects. However, initial ignition in the rich mixture led to high values of U_n, despite the high stretch rate (Figure 10). For ignitions with $\varphi_{ig} = 1.2$ in family A at 0.34 m/s, the initial burning velocity of the flame segment propagating in the lean mixture (t = 2 ms) was significantly higher than expected for lean stretched flames with $\varphi = 0.6$ and 0.7.

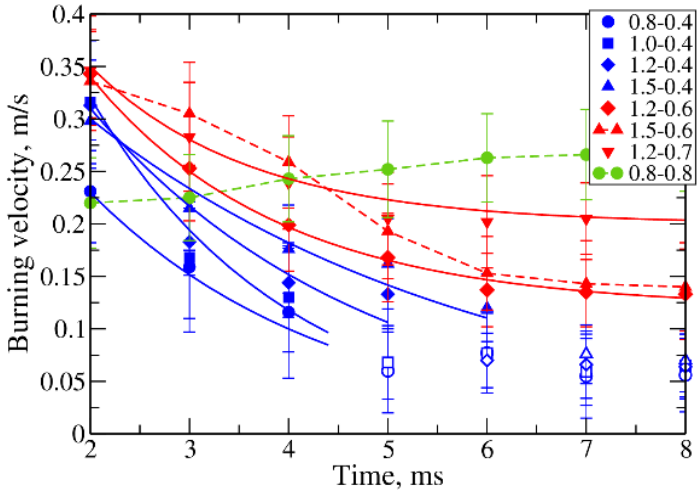

Fig 9 Burning velocity according to time: family A (red), family B (blue), and homogeneous flames (green) with φ=0.8. Extinguished flame conditions (open symbols)

For the two cases with $\varphi_{ig} = 1.2$, the velocity U_n showed identical time evolutions with an asymptotic trend of the exponential decrease for $t > 6\ ms$, where U_n was almost constant (Fig 9

and 10). The asymptotic values were close to those of the unstretched velocity, with 0.20 m/s for $\varphi_{ch} = 0.7$, and 0.14 m/s for $\varphi_{ch} = 0.6$.

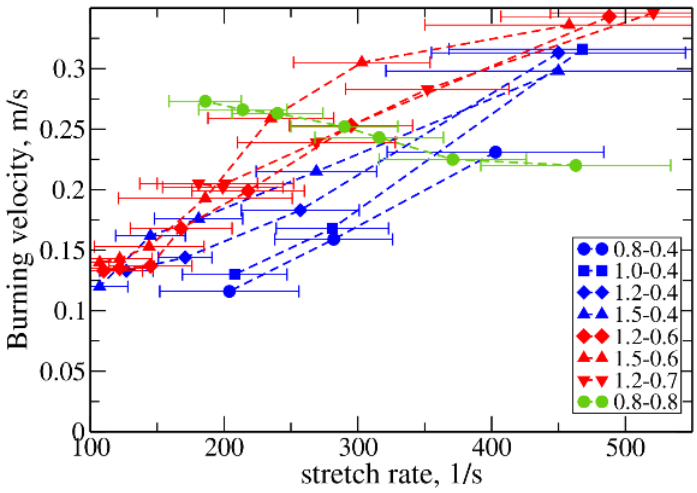

Fig 10 Burning velocity according to stretch rate

Table 2. *Exponential modeling of the burning velocity decay*

$$U_n(t-2) - U_\infty = \left(U_n(2ms) - U_\infty\right)e^{-\frac{t-2}{\tau}}$$

Family	$(\varphi_{ig} - \varphi_{ig})$	U_∞, m/s	$U_n(2\ ms)$, m/s	τ, ms
A	1.2–0.6	0.12	0.34	1.9
	1.2–0.7	0.2	0.35	1.6
B	1.5–0.4	0	0.3	4
	1.2–0.4	0	0.31	2.8
	1.0–0.4	0	0.32	2
	0.8–0.4	0	0.23	2.4

Exponential modeling of $U_n(t)$ (Table 2), from $t = 2\ ms$ to the asymptotic behavior, shows that the decay time was $1.6\ ms$ for $\varphi_{ch} = 0.7$, and $1.9\ ms$ for $\varphi_{ch} = 0.6$. The asymptotic behavior was attained more rapidly for $\varphi_{ch} = 0.7$ because of the lower stratification amplitude ($\varphi_{ig} = 1.2$ to $\varphi_{ch} = 0.7$).

Once the asymptotic behavior was attained (t>5 ms), a slight increase in U_n was observed for $\varphi_{ch} = 0.7$, corresponding to the decreasing stretch effect observed for increasing flame radii. For $\varphi_{ch} = 0.6$, the minimum value of U_n was very close to the value of U_n^*, and a slight decrease was observed, in agreement with previous observations by Balusamy et al. (Balusamy, Cessou and Lecordier 2014). This behavior illustrated the competition between the stretch effects, which tended to reduce the burning rate and the back-support behavior of the flame. After igniting in the homogeneous mixture with $\varphi_{ch} = 0.6$, outwardly propagating spherical flames were no

longer able to self-propagate due to overly intense stretch effects occurring with small flame radii. In the stratified case $(\varphi_{ig} = 1.2 \text{ to } \varphi_{ch} = 0.6)$ the flame succeeded to propagate despite its small radius, as confirmed by the OH gradient values (Figure 11), which were higher than the defined extinction threshold (17 000 a.u./mm). The flame was sustained by the memory effect, but was slowed down by the stretch effects. The gain provided by the memory effect decreased with time, and the influence of the stretch effect also decreased, resulting in a relatively constant burning velocity: for the investigated time range, the two effects were balanced, with a slightly faster decay observed for the memory effect.

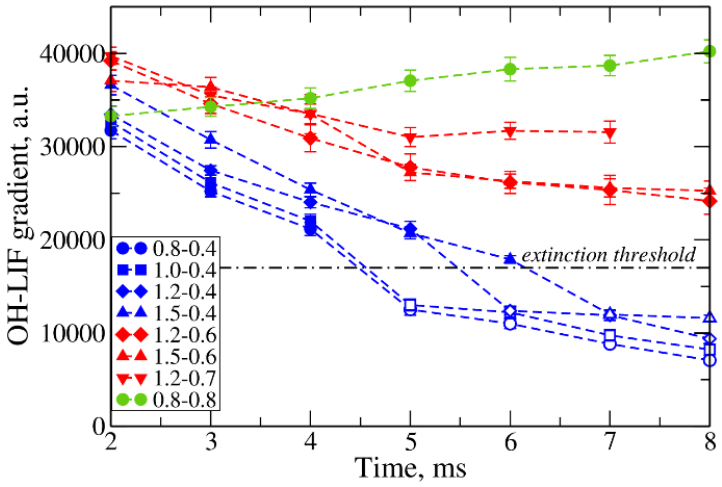

Fig 11 OH-PLIF gradient according to time

Overall, these results show that ignition in a slightly rich mixture resulted in a flame that rapidly propagated in the lean mixture despite the high stretch rates. This velocity decreased as the flame propagated in the lean mixture, with a decay time of slightly less than 2 ms. This high burning velocity was related to the discrepancy between the local equivalence ratio in the flame front (peak heat release) and in fresh gas. The flame propagation then adopted an asymptotic behavior with a burning velocity close to the fundamental velocity. The physical properties of the burned gas (here, mainly the high temperature) compensated for the non-equidiffusive effects of the lean stretched propane–air flame, which resulted in a leaner mixture in front of the flame with a lower burned gas temperature.

These observations were made for stratifications that led to few partial oxidation products in burned gas (peak equivalence ratio of 1.2). For $\varphi_{ig} = 1.5 \text{ to } \varphi_{ch} = 0.6$ partial oxidation products are more abundant in burned gas. At 2 ms, just after the flame had left the stratified layer, U_n was equal to 0.33 m/s, which is roughly the same value as for $\varphi_{ig} = 1.2 \text{ to } \varphi_{ch} = 0.6$ and for

$\varphi_{ig} = 1.2$ to $\varphi_{ch} = 0.7$. Because stretch had an effect on the flame, these identical velocities possibly indicate either an identical equivalence ratio within the flame front for the three cases, or a much richer flame whose burning velocity was increased by the stretch effects. The time decay was slower and differed from the exponential decay observed for the two other cases of family A. The concavity of the curve $U_n(t)$ differed from the ignition cases with $\varphi_{ig} = 1.2$, demonstrating that the burning velocity increased more strongly between 3 and 6 ms. This additional combustion enhancement is visible in Figure 10, in which the case $\varphi_{ig} = 1.5$ to $\varphi_{ch} = 0.6$ represents a faster burning velocity for stretch rates in a time range of 3 to 6 ms. These results show that the back-support behavior of the flame was enhanced by ignition in a richer stratified layer: the excess in partial oxidation products in burned gas enriched the flame front for longer and/or led to a secondary reaction in the burned gas (Haworth 2000). Due to the relative change in the curve concavity $U_n(t)$, a decay time cannot be determined through exponential modeling. However, the same asymptotic behavior as for $\varphi_{ig} = 1.2$ to $\varphi_{ch} = 0.6$ was attained after a slightly longer time (t>6 ms); this behavior was observed for all measured properties.

For the three cases of family A, the flame thickness δ_{LIF} showed the same time evolution. At $t = 2\ ms$, despite the lean mixture in fresh gas, the flame was relatively thin with a thickness close to the minimum value measured in near-stoichiometric homogeneous flames for the cases $\varphi_{ig} = 1.2$ to $\varphi_{ch} = 0.7$ and $\varphi_{ig} = 1.5$ to $\varphi_{ch} = 0.6$; the flame was slightly thicker for the case $\varphi_{ig} = 1.2$to $\varphi_{ch} = 0.6$ with $\delta_{LIF} = 400\ \mu m$, corresponding to $\varphi = 0.85$ for a homogeneous flame (Figure 1). These smaller thickness values are consistent with high values of U_n. Then, δ_{LIF} increased over time to attain a roughly constant value close to that measured in the homogeneous flame with $\varphi_{ch} = 0.6$ and 0.7 (Figure 7).

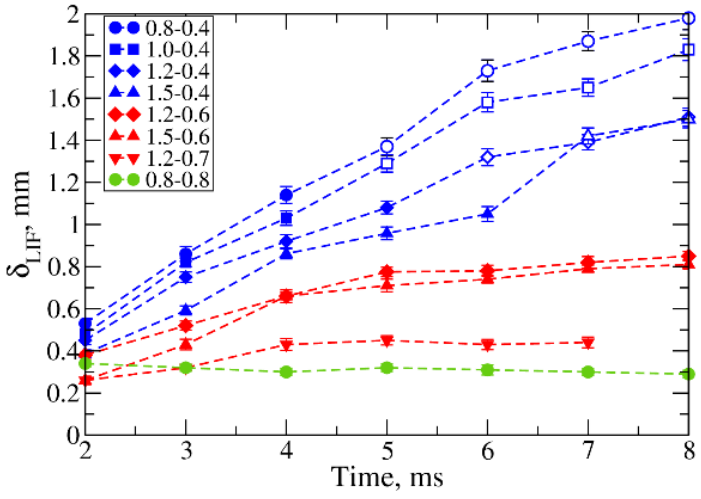

Fig 12 Flame thickness δ_{LIF} according to time

Family B: propagation in a lean nonflammable mixture

Flames of family B, for which the lean mixture was below the flammability limit, were investigated to determine whether this combustion enhancement also occurred in nonflammable mixtures and over which time scales. For these four flames, the OH-LIF gradient was used to differentiate the border of hot burned gas from the active flame front (Fig 11). A $t = 2\ ms$, the OH-LIF gradient values were much higher than the extinction threshold (17 000 a.u./mm). Depending on the stratification amplitude, the gradient's progressive decay and the extinction occurred at different times (all of which were greater than 4 ms) and increased with the equivalence ratio at ignition. Thus, ignition in a richer stratified mixture allowed the flame to propagate in the nonflammable mixture: the flame ignited in the lean mixture ($\varphi_{ig} = 0.8$) as well as in the rich mixture ($\varphi_{ig} = 1.5$). Figure 9 shows the burning velocities over time for active reaction zones (with an OH-LIF gradient higher than 17 000 a.u/mm.). The conditions for which the flame extinguished (open symbols in Figure 5), indicate that the burning velocity was non-zero due to measurement inadequacies in this case. At 2 ms, the case $\varphi_{ig} = 0.8$ to $\varphi_{ch} = 0.4$ had a burning velocity of 23 cm/s, a value close to the velocity measured for φ_{ig}= 0.8 to $\varphi_{ch} =$ 0.8 (Fig 9), which is evidence of enhanced combustion in the nonflammable mixture. This increase was observed even if the flame was ignited in a lean stratified layer (peak equivalence ratio of 0.8). In this case, enhanced combustion could only have resulted from an increase in the burned gas temperature. This enhancement decreased over time, and flame extinction occurred between 4 and 5 ms. The three other flames (φ_{ig} = 1.0 to $\varphi_{ch} =$ 0.4; $\varphi_{ig} =$ 1.2 to $\varphi_{ch} =$ 0.4; and $\varphi_{ig} =$1.5 to $\varphi_{ch} =$ 0.4) had nearly identical burning velocities of around 0.3 m/s at 2 ms. The burning velocities decreased over time; the slowest decay time was observed with the richer stratification. Exponential modeling of the decay with $U_\infty = 0\ m/s$ took into account the extinction occurrence. The following decay times were determined: 4 ms for $\varphi_{ig} = 1.5$ to $\varphi_{ch} = 0.4$; 2.8 ms for $\varphi_{ig} = 1.2$ to $\varphi_{ch} = 0.4$; and 2 ms for $\varphi_{ig} = 1.0$ to $\varphi_{ch} = 0.4$ (Table 2). For φ_{ig} = 0.8 to $\varphi_{ch} =$ 0.4 the decay time was slightly longer (2.4 ms), or at least roughly equivalent, considering the measurement uncertainty. This result demonstrates the combined effects of stretch and stratification. For rich propane–air mixtures, stretching tended to increase the burning velocity. Thus, in these cases, combustion was enhanced by both stratification and stretch, which led to higher burned gas temperatures. During propagation in the lean mixture, these positive influences decreased simultaneously. For ignition in the lean mixture with φ_{ig} = 0.8 to $\varphi_{ch} =$ 0.4, the burned gas temperature increased as a result of ignition in the stratified mixture, whereas stretch tend to decrease this temperature. During propagation in the lean mixture, the effect of stretch on combustion decreased progressively, leading to a

slower decay. However, the increase in decay time remained moderate, and the flame was rapidly extinguished (t<5 ms) because of the minor presence of a back-support structure for the stratification in this case.

The combustion enhancement was also noticeable with the small values of δ_{LIF} at 2 ms (Fig 12). The flame thickness was around 500 µm, and was as thin as 400 µm for $\varphi_{ig} = 1.5$ to $\varphi_{ch} = 0.4$. These values are close to the value measured in a homogeneous flame with $\varphi = 0.8$. The flame became thicker over time, and extinction occurred at $\delta_{LIF} > 1.2\ mm$. For the entire duration, the richer the stratification was, the thinner the flame became. Additionally, for a given stretch rate, the fastest burning velocity occurred in the richer stratification (Fig 10). These results show that a richer stratification resulted in an increased and longer combustion enhancement in the lean nonflammable mixture.

4 Conclusion

Simultaneous PIV, anisole-PLIF, and OH-PLIF measurements were used to experimentally investigate the possibility of lean-burn combustion. Outwardly propagating flames were ignited under laminar stratification conditions generated in a constant volume vessel. After ignition in a rich stratified layer, the flame properties (burning velocity, stretch, thermal thickness δ_{LIF}) were analyzed in a lean flammable mixture bordering on the flammability domain (family A) and in a nonflammable mixture (family B).

The behavior of flames in family A showed that the lean-mixture flames benefited from ignition in the rich stratified layer, which led to faster burning velocities despite the high stretch rate that usually inhibits combustion in such a lean mixture ($\varphi = 0.6$). The burning velocity decreased toward fundamental values, with a decay time close to 2 ms for the investigated configuration. The memory effect compensated for the stretch effect, resulting in a fundamental burning velocity at a non-zero stretch rate. For family B, the flame maintained an active flame front in the nonflammable mixture over time, which increased with the equivalence ratio in the stratification. The combustion enhancement was also apparent in the flame thickness values δ_{LIF}: the flame became thinner in the early stage of propagation in the lean mixture. The thickness values were depended on the effective equivalence ratio in the flame front and on the flame thickness, whereas the burning velocity decreased. Stratified flames were used to construct a database suitable for validating numerical simulations and investigating the influence of—in contrast to homogeneous combustion—higher burned gas temperatures and excess in partial combustion products, which could enrich the flame front and compensate for the negative thermodiffusive effects of the lean propane flame (Le<1).

5 Acknowledgment

We gratefully acknowledge the support of the French *Agence Nationale de la Recherche* [National Research Agency] (ANR) and the French *Centre National de la Recherche Scientifique* [National Center for Scientific Research] (CNRS) through the ACTING-CO2 program, provided in collaboration with the French engine research grouping *Groupement Scientifique Moteurs* (GSM). We would like to thank Dr Ghislain Lartigue for his help in modeling the flame and for the fruitful discussions.

6 References

Andrews GE, Bradley D (1972) The burning velocity of methane-air mixtures. Combust Flame 19:275-288 DOI http://dx.doi.org/10.1016/S0010-2180(72)80218-9

Balusamy S, Cessou A, Lecordier B (2011) Direct measurement of local instantaneous laminar burning velocity by a new PIV algorithm. Experiments in Fluids 50:1109-1121

Balusamy S, Cessou A, Lecordier B (2014) Laminar propagation of lean premixed flames ignited in stratified mixture. Combust Flame 161:427-437 DOI http://dx.doi.org/10.1016/j.combustflame.2013.08.023

Bayley AE, Hardalupas Y, Taylor AMKP (2010) Curvature measurements of a lean partially-premixed model gas turbine combustor 15th Int Symp on Applications of Laser Techniques to Fluid Mechanics. Lisbon, Portugal,

Bradley D, Gaskell, P.H., Gu, X.J., (1996) Burning Velocities, Markstein Lengths, and Flame Quenching for Spherical Methane-Air Flames: A Computational Study. Combust Flame 104:176-198

Egolfopoulos FN, Hansen N, Ju Y, Kohse-Höinghaus K, Law CK, Qi F (2014) Advances and challenges in laminar flame experiments and implications for combustion chemistry. Progress in Energy and Combustion Science 43:36-67 DOI http://dx.doi.org/10.1016/j.pecs.2014.04.004

Goodwin DG, Moffat HK, Speth RL (2015) Cantera: An Object-oriented Software Toolkit for Chemical Kinetics, Thermodynamics, and Transport Processes Cantera: An Object-oriented Software Toolkit for Chemical Kinetics, Thermodynamics, and Transport Processes. Version 2.2.0 edn.,

Haworth DC, Blint, R.J., Cuenot, B., Poinsot, T.J., (2000) Numerical Simulation of Turbulent Propane-Air Combustion with Nonhomogeneous Reactants. Combust Flame 121:395-417

Jerzembeck S, Peters N, Pepiot-Desjardins P, Pitsch H (2009) Laminar burning velocities at high pressure for primary reference fuels and gasoline: Experimental and numerical investigation. Combust Flame 156:292-301 DOI 10.1016/j.combustflame.2008.11.009

Jiménez C, Cuenot, B., Poinsot, T., Haworth, D., (2002) Numerical Simulation and Modeling for Lean Stratified Propane-Air Flames. Combust Flame 128:1-21

Kang T, Kyritsis DC (2007) Departure from quasi-homogeneity during laminar flame propagation in lean, compositionally stratified methane–air mixtures. Proc Comb Inst 31:1075-1083 DOI 10.1016/j.proci.2006.07.051

Marzouk YM, Ghoniem AF, Najm HN (2000) Dynamic response of strained premixed flames to equivalence ratio gradients. Proc Comb Inst 28:1859-1866 DOI 10.1016/s0082-0784(00)80589-5

Nowakowska M, Herbinet O, Dufour A, Glaude P-A (2014) Detailed kinetic study of anisole pyrolysis and oxidation to understand tar formation during biomass combustion and gasification. Combust Flame 161:1474-1488 DOI http://dx.doi.org/10.1016/j.combustflame.2013.11.024

Pires da Cruz A, Dean, A.M., Grenda, J.M., (2000) A Numerical Study of the Laminar Flame Speed of Stratified Methane/Air Flames. Proc Combust Inst 28:1925-1932

Richardson ES, Granet VE, Eyssartier A, Chen JH (2010) Effects of equivalence ratio variation on lean, stratified methane-air laminar counterflow flames. Combustion Theory and Modelling 14:775 - 792

Sadanandan R, Stöhr M, Meier W (2008) Simultaneous OH-PLIF and PIV measurements in a gas turbine model combustor. Applied Physics B 90:609-618 DOI 10.1007/s00340-007-2928-8

Sweeney M, Hochgreb S (2009) Autonomous extraction of optimal flame fronts in OH planar laser-induced fluorescence images. Appl Opt 48:3866-3877 DOI 10.1364/ao.48.003866

Zhou RG, Hochgreb S (2013) The behaviour of laminar stratified methane/air flames in counterflow. Combust Flame 160:1070-1082 DOI 10.1016/j.combustflame.2013.01.023